

Supporting information

Rapid spread, slow evaporation: long-lasting water film on hydrogel nanowire arrays for continuous wearables

Peijia Li^{1,4}, Yilin Wang^{1,4}, Ming Qiu¹, Yixiao Wang¹, Zhaoxiang Lu², Jianning Yu¹, Fan Xia³, Yun Feng^{2*}, Ye Tian^{1,4,5*}

¹ Laboratory of Bio-Inspired Materials and Interface Sciences, Technical Institute of Physics and Chemistry, Chinese Academy of Sciences, Beijing 100190, China

² Department of Ophthalmology, Peking University Third Hospital, Beijing 100191, China

³ State Key Laboratory of Biogeology and Environmental Geology, Faculty of Materials Science and Chemistry, China University of Geosciences, Wuhan 430078, China

⁴ School of Future Technology, University of Chinese Academy of Sciences, Beijing 100049, China

⁵ Suzhou Institute for Advanced Research, University of Science and Technology of China, Jiangsu 215123, China

*Corresponding author. E-mail: fengyun@bjmu.edu.cn; tianyely@iccas.ac.cn

Content list

Materials and methods

Supplementary Figure 1. SEM image of healthy and dry corneas surface of the rabbits.

Supplementary Figure 2. Schematic of HNWs surface modification to form TE@HNWs.

Supplementary Figure 3. The frontal SEM images of the HNWs with different length nanowire arrays.

Supplementary Figure 4. The ATR-FTIR spectra of HNWs (gray) and TE@HNWs (blue).

Supplementary Figure 5. The dynamic spreading behavior of 0.1% TE@HNWs on 3 μm nanowire arrays at different pHs.

Supplementary Figure 6. The CA snapshots of water droplet on TE@HNWs surfaces of different TE concentration.

Supplementary Figure 7. The CA snapshots and dynamic spreading processes of 2 μL droplet on 0.5% TE@HNWs surface.

Supplementary Figure 8. The changes of the edge of water film on 0.5% TE@HNWs surface.

Supplementary Figure 9. The spreading behavior of TE@HNWs (a) and TE@flat (b) at different TE concentrations.

Supplementary Figure 10. The mass change of 2 μL water droplets on different surfaces.

Supplementary Figure 11. Phase change behaviors and the mobility of hydrated water state in different hydrogel surfaces.

Supplementary Figure 12. The basic indicator of hydrogel lenses.

Supplementary Figure 13. Oil adhesion of the hydrogel lenses.

Supplementary Figure 14. Friction stability of the hydrogel lenses.

Supplementary Figure 15. Biocompatibility of the TE@HNWs lenses.

Supplementary Table 1. Monomers ratio for the fabrication of silicone hydrogel.

1. Materials and methods

1.1 Morphological observation of rabbit corneal epithelial cells

Female New Zealand white rabbits (2.2-2.5kg) are purchased from Beijing Jinnuyang Laboratory Animal Breeding Co., Ltd. Animal procedures for the rabbit experiments are reviewed and approved by the Experimental Animal Ethics Committee, Peking University Third Clinical School of Medicine, China. All experiments are performed in compliance with the guidelines for protecting animal welfare and implementing improvement plans to euthanize animals. Rabbits are killed via a systemic injection of sodium pentobarbital under deep anesthesia, followed by peeling off the entire cornea, which is stored in the PBS buffer.

In order to obtain the correct and complete morphology of rabbit corneal epithelial cells, the cornea was treated by gradient dehydration and critical drying. Firstly, the corneal cells were immobilized by soaking the sample with glutaraldehyde for 12h. Then, suck out glutaraldehyde and rinse with deionized water for 3 times. Next, 50 %, 70 %, 85 %, 95 % and 100 % ethanol gradients are used for dehydration. Finally, the dry samples are obtained by critical point drying and deethanolization for 1h. The morphology of corneal epithelial cells was observed by scanning electron microscopy (SEM) after sputtering gold.

1.2 Fabrication of the HNWs

SiM (98%), NVP, 2-hydroxyethyl methacrylate (HEMA), photoinitiator 2-hydroxy-2-methylbenzene acetone (D-1173), and crosslinking agent poly (ethylene glycol) dimethacrylate (PEGDMA, average Mn 750) are added into flask in orders, followed use nitrogen to remove excess oxygen. Then, the mixture was added onto AAO mold (Shanghai Shang-Mu Nano Technology, Ltd.) and cured by an LED UV curing system (UPP3- 734, Utata) for 10 min at room temperature. The copolymer and the mold are hydrated in water for 5 h. Finally, $\text{CuCl}_2/\text{NaOH}$ solution are used in turn to dissolve the AAO templates.

1.3 Fabrication of the TE@HNWs

Firstly, HNWs are oxidized by air plasma and then treated by mixed solution ($V_{H_2O}:V_{HCl}:V_{H_2O_2}, 5:1:1$) to generate enough superficial hydroxyl groups (-OH). Afterward, the coupling agent N-[(3-trimethoxysilyl) propyl]- ethylenediamine triacetic acid trisodium salt (TMS-EDTA, TE) is diluted to a certain concentration, and the HNWs are incubated in this solution at 50°C for 5 h. Finally, the TE macromolecules are firmly and covalently graft onto the HNWs, named as TE@HNWs.

1.4 Characterization of the morphology and dynamic spreading process

Morphology of the HNWs and TE@HNWs hydrogels is investigated by SEM (JEOL, JSM-7500F, Japan). The lateral-view dynamic spreading processes are measured with a contact-angle system (OCA 20, DataPhysics, Germany) at room temperature. The average spreading times are obtained by measuring three samples in three different positions.

1.5 Water Structure Monitored by ATR-FTIR Spectroscopy

The HNWs is laid on ZnSe crystal and pressed with a pressure pole. All ATR-FTIR spectra are recorded at 25 °C by an FTIR spectrometer (Excalibur 3100 with ZnSe ATR sampling accessory, The United States). The wavenumber range is from 4000 to 2800 cm^{-1} , the resolution was 8 cm^{-1} with 60 scans. Wire 5.1 software is used for spectrum data processing, and Gaussian function is used for peak fitting.

1.6 Melting behavior of samples by DSC measurement

The melting behavior of gel are observed by a differential scanning calorimeter (DSC). During the DSC measurement of the melting behavior, the TE@HNWs is closely sealed in an Al crucible to prevent the evaporation of water and kept at -25 °C for 5 min to be fully frozen. Then the measurement is performed with scans at linear heating rate 5 °C /min under nitrogen flow flux (50 mL/min), in the temperature range from -25 to 25 °C. To avoid the influence of bulk water on the surface, the deionized water of the TE@HNWs surface is wiped with paper before tested.

1.7 NMR measurements for water in samples

The proton spin-spin relaxation time (T₂) measurements of water in different hydrogel surface are carried out on a Bruker AV600 NMR spectrometer using the Carr-Purcell-Meiboom-Gill pulse sequence. A spacing of 1.2 ms between the 90° and 180° pulse is used.

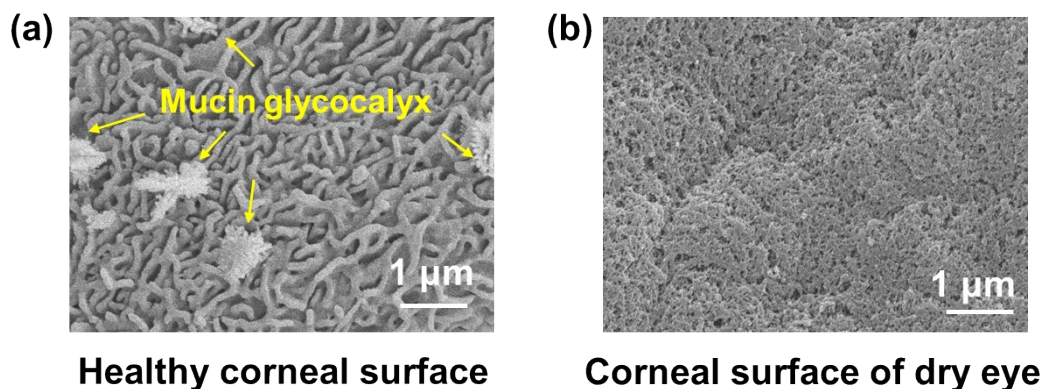
1.8 Characterization of the TE@HNWs as contact lenses

The oxygen permeability is determined using a permeability testing instrument (OX2, China) at a humidity of ≈100%. The light transmittance measurements are carried out with a UV–visible spectrophotometer at a wavelength range of 400–800 nm. Liquid paraffin is selected to mimic the lipid secretions on the ocular surface, and the paraffin oil adhesion is recorded by a high sensitivity micro-electromechanical balance system. The images of the adhered fluorescent-labeled protein (BSA, Guangdong Shun-Hao biotechnology Co., Ltd.) are obtained by a fluorescence microscope (Vision Engineering Co.). Commercial skin moisture detector with copper probe sensor monitors changes in surface moisture.

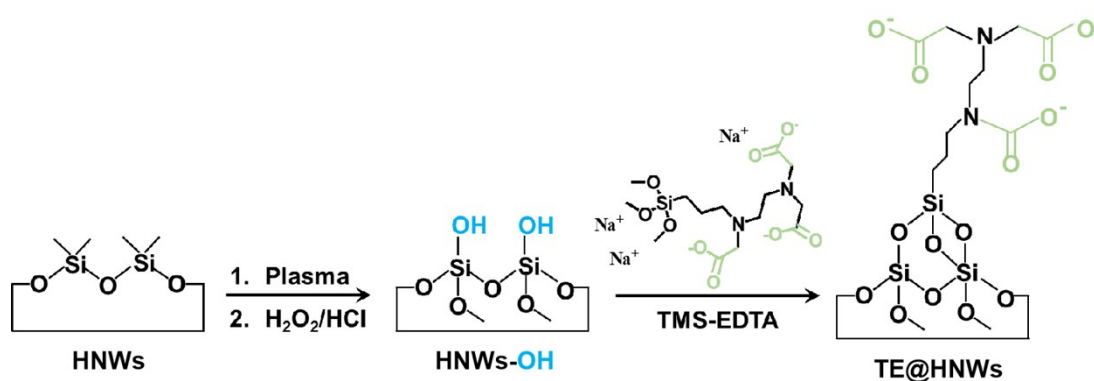
1.9 The biocompatibility of TE@HNWs lens assessed by *in vitro* cell culture experiments

To evaluate the biocompatibility of the TE@HNWs lenses, the human corneal epithelial cell viability is analysed by Cell Counting Kit-8 (CCK8, Dojindo, Japan) according to the manufacturer's protocols. Human corneal epithelial cells are seeded and cultured at a density of 5×10^3 /well in 100 uL of medium into 96-well microplates (Corning, USA). Then, the cells are treated with various lenses (TE@HNWs, HYDRON and Bausch & Lomb lenses). After treatment for 24 hours 10 uL of CCK-8 reagent is added to each well and then cultured for 2 hours. All experiments are performed in quadruplicate. The absorbance is analysed at 450 nm using a microplatereader (Bio-Rad, Hercules, CA, USA) using wells without cells as blanks. The proliferation of cells is expressed by the absorbance.

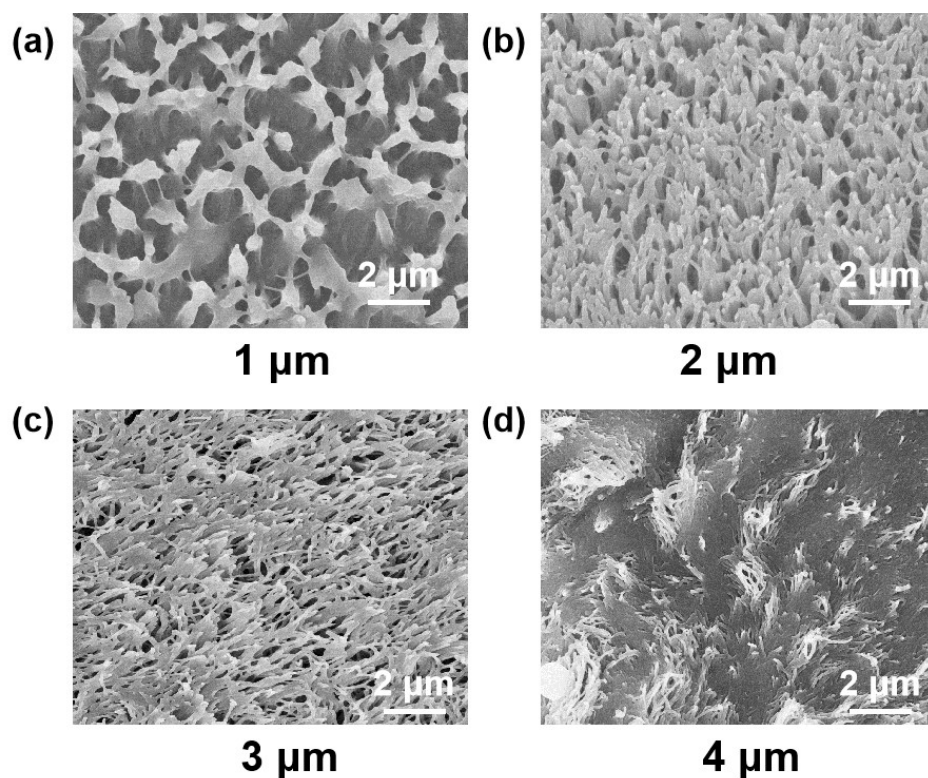
2. Figures



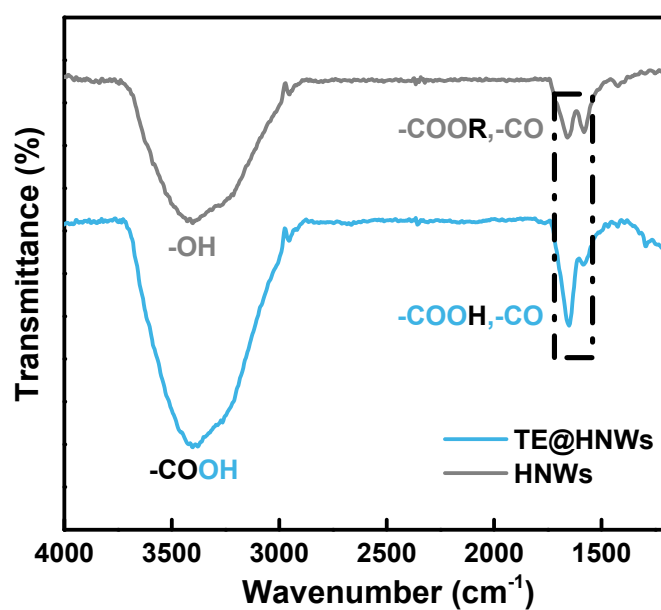
Supplementary Figure 1. SEM image of healthy and dry corneas surface of the rabbits. (a) Healthy corneal epithelial cells are covered with nanowire arrays and the mucin glyocalyx, and (b) the nanowire and mucin in the dry cornea surface are severely damaged.



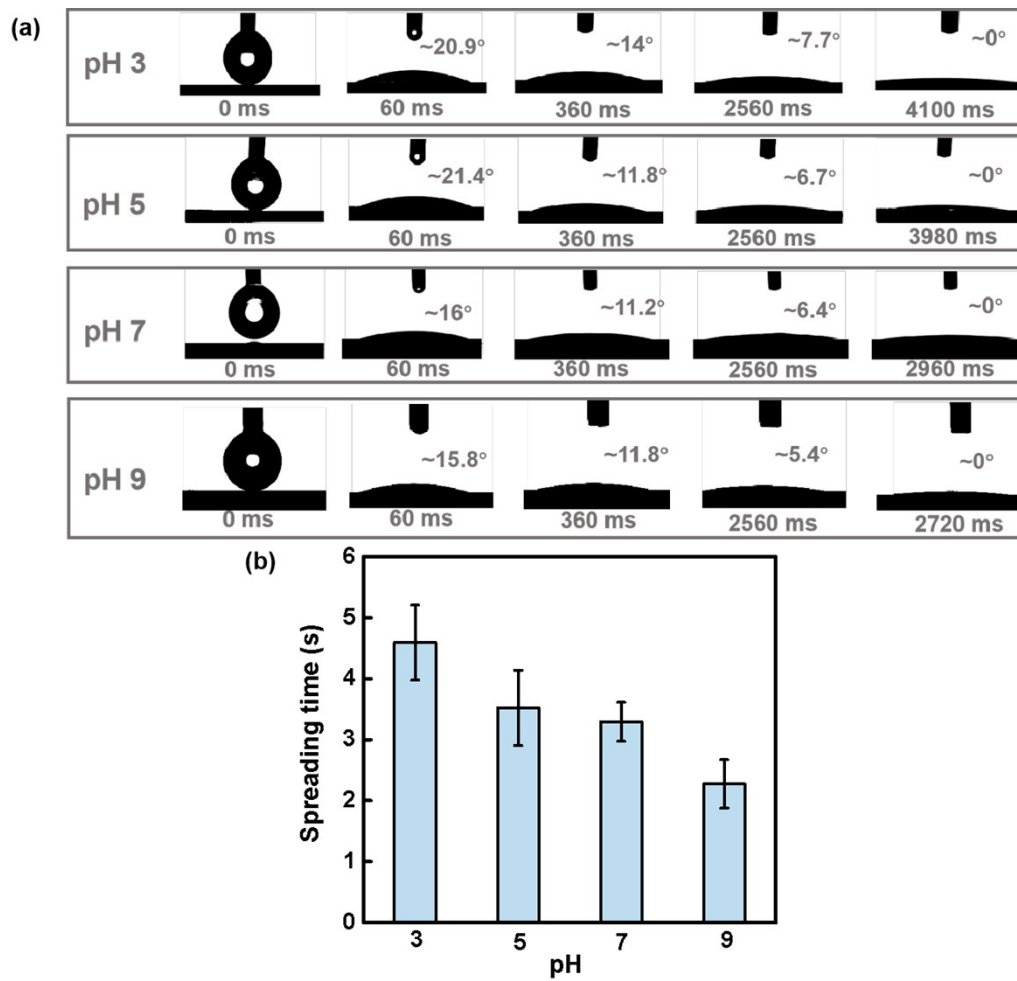
Supplementary Figure 2. Schematic of HNWs surface modification to form TE@HNWs. It mainly includes the following two key steps: chemical modification of HNWs surface formation of superficial hydroxyl groups and silanization grafting of TMS-EDTA.



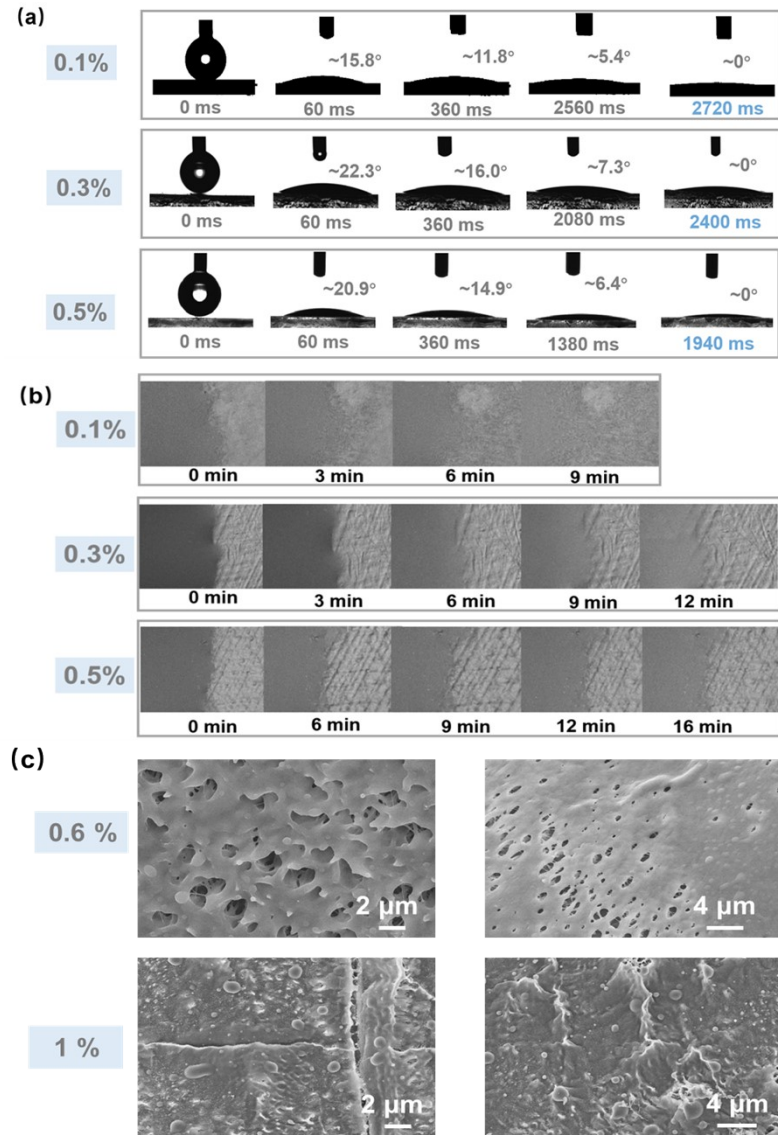
Supplementary Figure 3. The frontal SEM images of the HNWs with different length nanowire arrays. (a-d) The lengths of HNWs nanowire are ~ 1 , ~ 2 , ~ 3 and ~ 4 μm , respectively. It is obvious that 3 μm nanowire arrays is more dispersed than 1 and 2 μm nanowire arrays. And the 4 μm nanowire arrays collapses severely.



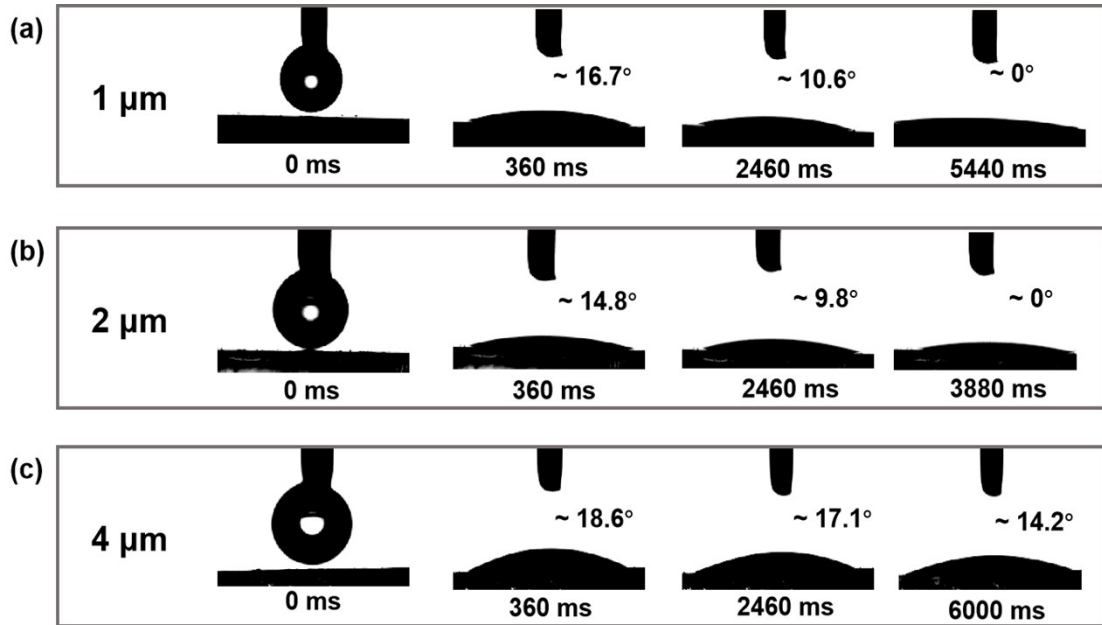
Supplementary Figure 4. The ATR-FTIR spectra of HNWs (gray) and TE@HNWs (blue).



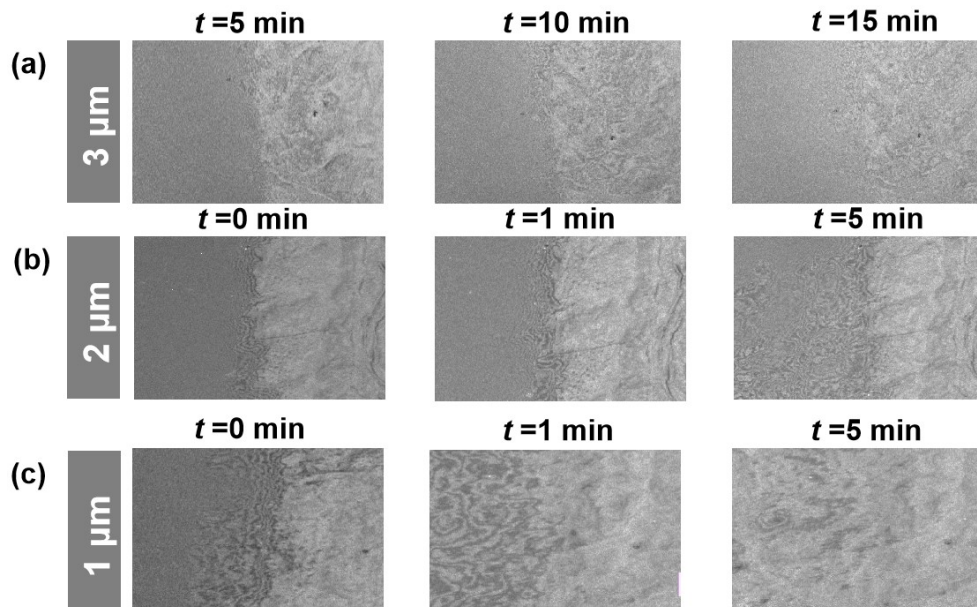
Supplementary Figure 5. The dynamic spreading behavior of 0.1% TE@HNWs on 3 μm nanowire arrays at different pHs. A 2 μL water droplet spreads faster at higher pHs, and the fastest speed is at pH 9.



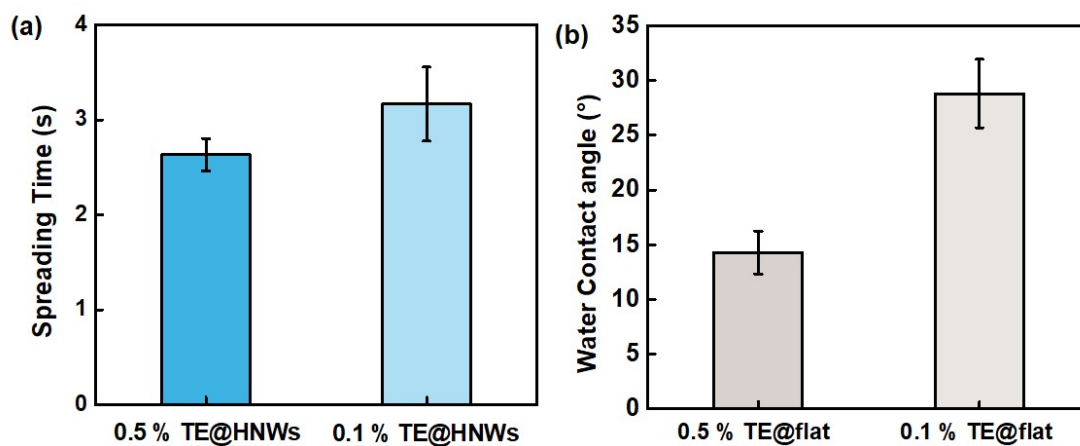
Supplementary Figure 6. The CA snapshots of water droplet on TE@HNWs surfaces of different TE concentration (a) and the optical images of the edge of water film at different time (b). And SEM images show that the nanowires are covered at 0.6% and 1% TE concentrations (c).



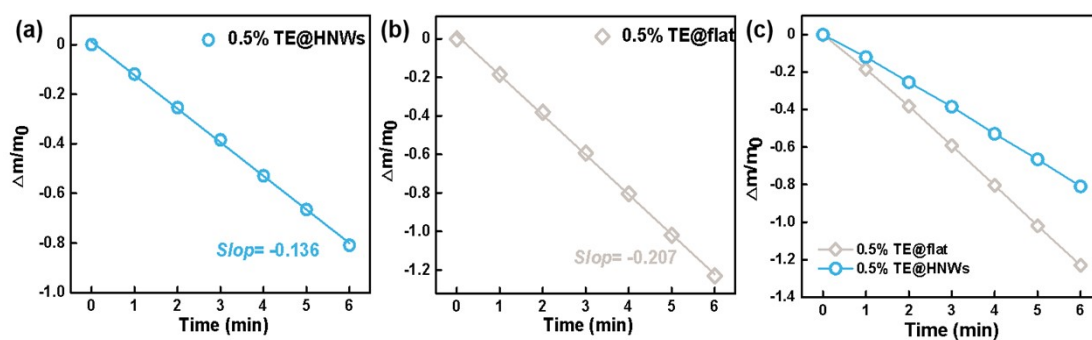
Supplementary Figure 7. The CA snapshots and dynamic spreading processes of 2 μL droplet on 0.5% TE@HNWs surface. A droplet can spread out within 5.44 s on 1 μm nanowire arrays until the CA approaches $\sim 0^\circ$ (a), and a same volume droplet is able to spread out within 3.88 s on 2 μm nanowire arrays (b). While on 4 μm nanowire arrays, spreading is stopped at 6 s (c), which is because the nanowire collapse is similar to the flat surface.



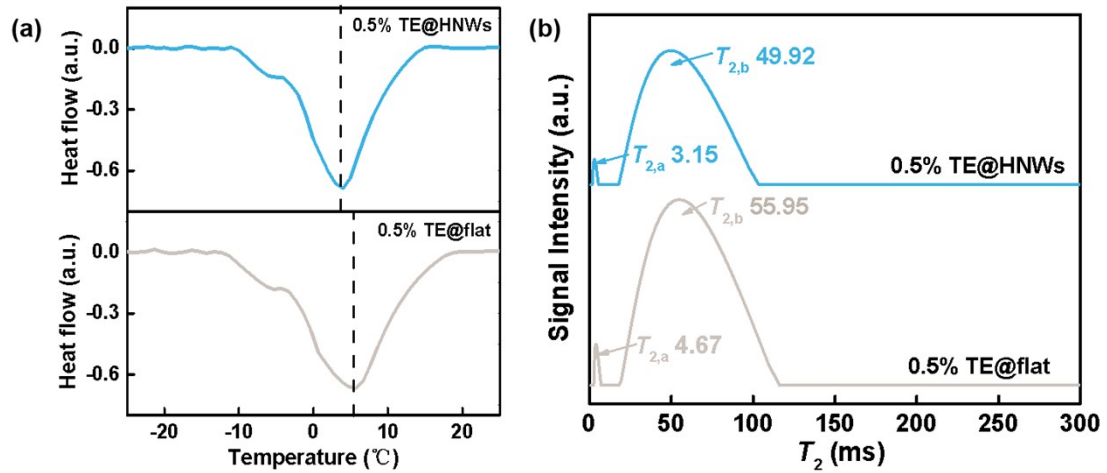
Supplementary Figure 8. The changes of the edge of water film on 0.5% TE@HNWs surface. (a) The water film is no obvious rupture within 10 min on 3 μm nanowire arrays, while on 1 and 2 μm nanowire arrays, unstable streaks appear within 1 min (b) and (c).



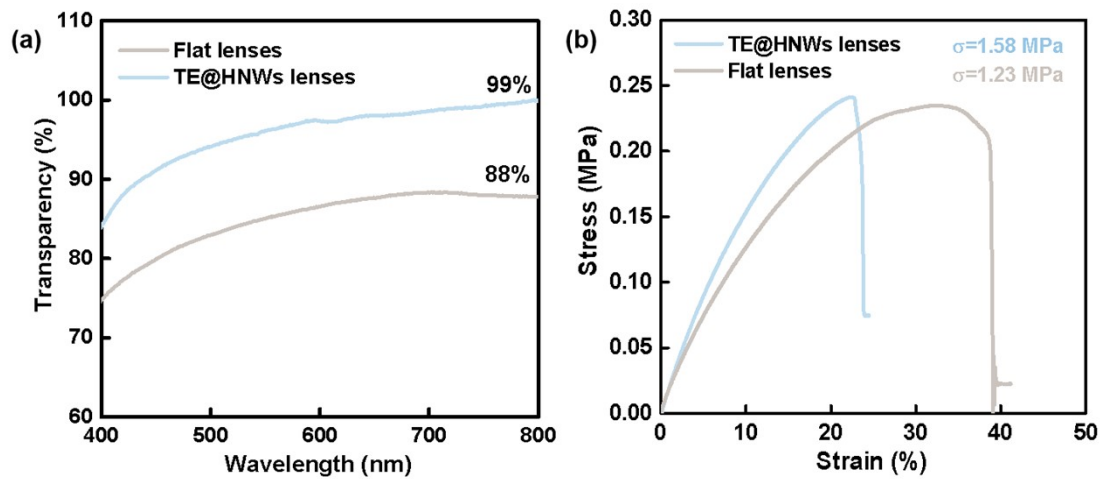
Supplementary Figure 9. The spreading behavior of TE@HNWs (a) and TE@flat (b) at different TE concentrations.



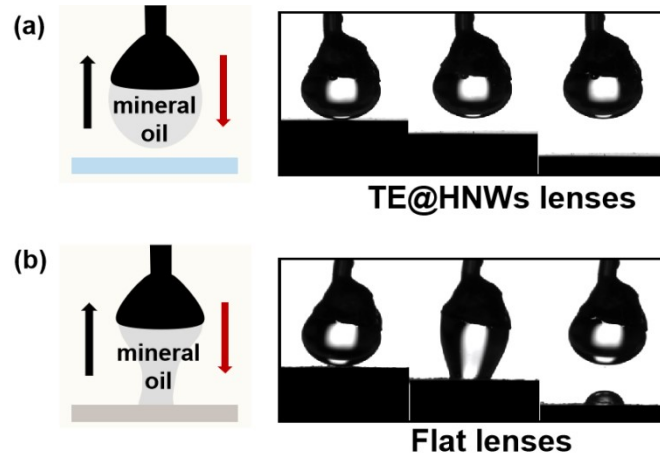
Supplementary Figure 10. The mass change of 2 μ L water droplets on different surfaces. (a) 0.5% TE@HNWs, (b) 0.5% TE@flat and water evaporates more slowly on 0.5% TE@HNWs (c).



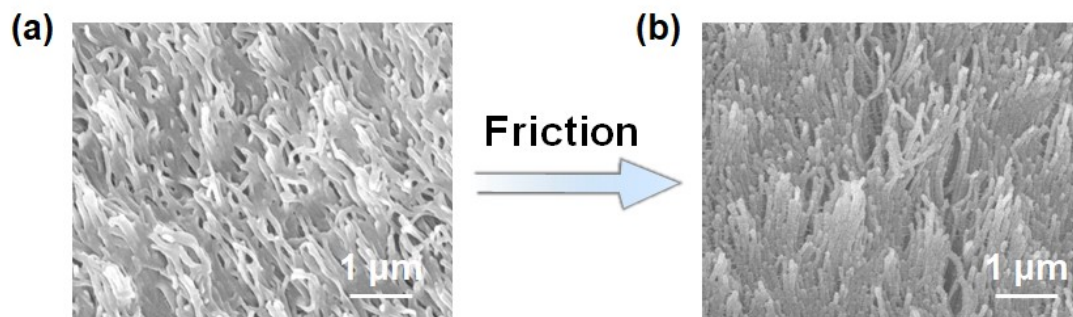
Supplementary Figure 11. Phase change behaviors and the mobility of hydrated water state in different hydrogel surfaces. (a) DSC curves of the melting behavior of water frozen and (b) T₂ decay curves of water on 0.5% TE@HNWs and 0.5% TE@flat surfaces.



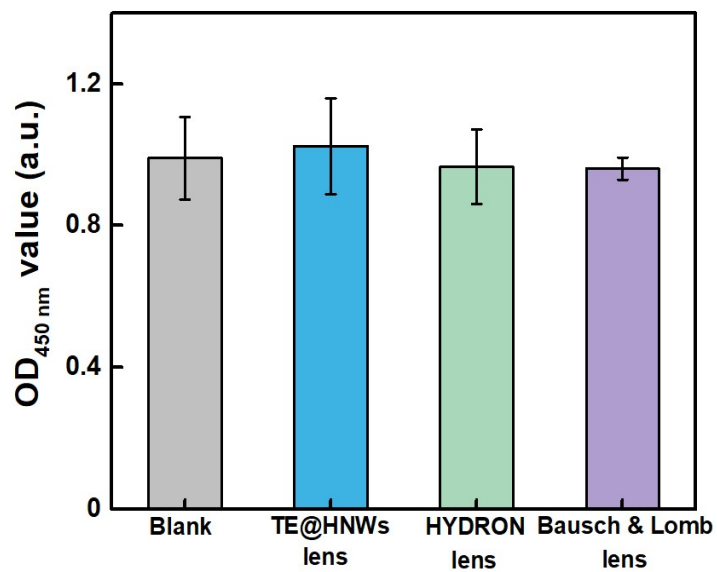
Supplementary Figure 12. The basic indicator of hydrogel lenses. The transparency (a) and the stress-strain curve (b) of different hydrogel lenses.



Supplementary Figure 13. Oil adhesion of the hydrogel lenses. (a), (b) the corresponding snapshots of the receding process which shows the mineral oil is strongly attached to flat lenses.



Supplementary Figure 14. Friction stability of the hydrogel lenses. It can be seen from the SEM images before (a) and after (b) friction that the morphology of the nanowire array remains intact without obvious damage. Simulated blinking friction condition: the friction speed is 3 mm/s, the cycle time is 10000 s, and the pressure is 40 nm.



Supplementary Figure 15. Biocompatibility of the TE@HNWs lenses. The absorbance of the TE@HNWs at 450 nm measured by the enzyme-labeled instrument has a stable and high OD value.

Supplementary table 1. Monomers ratio for the fabrication of silicone hydrogel.

Component	w (%)	CA	Q_{wc}	Character
SiM/NVP/HEMA/EGDMA	30/60/10/4	73.6°	56.9 %	soft
	30/60/10/6	71.5°	61.2 %	soft
	30/50/20/4	86.5°	34.2 %	hard
	30/50/20/6	84.6°	34.9 %	hard